

1 Article

2 Numerical Study on the Dynamic Behavior of a 3 Francis Turbine Runner Model with a Crack

4 Ming Zhang^{1,*}, Xingfang Zhang² and Weiqiang Zhao¹

5 ¹ Center for Industrial Diagnostics and Fluid Dynamics (CDIF), Polytechnic University of Catalonia (UPC).

6 Av. Diagonal, 647, ETSEIB, Barcelona, CO 08028 Spain; ming.zhang@upc.edu; weiqiang.zhao@upc.edu

7 ² College of Chemistry and Chemical Engineering, Taiyuan University of Technology, Taiyuan, CO 030024,
8 China; zxftut@163.com

9 * Correspondence: ming.zhang@upc.edu; Tel.: +34-657-277-255

10

11 **Abstract:** The crack in the blade is the most common type of fatigue damage for Francis turbines.
12 However, the crack sometimes is difficult to be detected in time using the current monitoring system
13 even when the crack is very large. To better monitor the crack, it is imperative to research the effect
14 of a crack on the dynamic behavior of a Francis turbine. In this paper, the dynamic behavior of a
15 Francis turbine runner model with a crack was researched numerically. The intact numerical model
16 was first validated by the experimental data available. Then, a crack was created at the intersection
17 line between one blade and the crown. The change in dynamic behavior with increasing crack length
18 was investigated. Crack-induced vibration localization theory was used to explain the dynamic
19 behavior changes due to the crack. Modal analysis showed that the adopted theory could basically
20 explain the modal behavior change due to the crack. The FFT results of the modal shapes and the
21 localization factors (LF) were used to explain the forced response changes due to the crack. Based
22 on the above analysis, the challenge of crack monitoring was analyzed. This research can also
23 provide some references for more advanced monitoring technologies.

24 **Keywords:** Francis turbine, crack, dynamic behavior, vibration localization, lumped parameter
25 mode, localization factor, forced response.

26

27 1. Introduction

28 The Francis turbines is one type of widely used hydraulic turbine. Due to the higher head, more
29 frequent extreme off-design operations and a reduced ratio of thickness/weight in runners currently
30 as well as occasional small material flaws, many cases of Francis turbine failure have been reported
31 in the literature [1-3]. Cracking is the most common type of damage in daily operations. A large crack
32 usually originates from a very small crack or flaw, which is usually undetectable by the current
33 monitoring system, and it will continuously grow under hydraulic dynamic force. If this crack is not
34 detected in time, catastrophic failure to the machine may occur [1, 4]. Figure 1 is a Francis turbine
35 blade failure case reported by [2], in which a large crack occurred on one blade to cause it to nearly
36 break off before being detected. This failure case also indicates the challenge of crack monitoring in
37 the Francis turbine. To better monitor this type of crack, it is imperative to research the dynamic
38 behavior of the runner with a crack.

39

40 The dynamic behaviors of Francis turbine have been widely researched in the literature [5, 6].
41 However, most of these studies were conducted on the intact runners, and the studies on the runners
42 with crack are very few. In fact, Francis turbine can be seen as one type of bladed-disk structure (or
43 one-dimensional cyclic system[7, 8]). Though it seems the geometries of the band and crown are very
44 different from the disk of the traditional bladed-disk structures, from the theoretical viewpoint, there
45 are no essential differences between them. For bladed-disk structures with crack, the well-known

46 vibration localization can occur, which has been used for crack monitoring in many other types of
47 turbines[9-12]. The vibration localization in Francis turbine has been studied very limitedly in the
48 literature. Shuai Wang [13] researched the effect of crack on a pump-turbine like centrifugal impeller
49 from the viewpoint of the vibration localization in bladed-disk structures. However, the information
50 still is limited.

51



52
53 Figure 1. Francis turbine blade failure case reported by D Frunzăverde, 2010[2].
54

55 Generally, for traditional bladed-disk structures the crack has a more significant influence on
56 blades dominated modes due to the lower coupling stiffness and causes some modes quickly
57 localized to the damaged blade. This is the reason why most of researches focus on blade-dominated
58 modes [9-12]. For the strongly localized mode, the frequency quickly deviates from the original tuned
59 frequency. Therefore, this natural frequency deviations and forced response changes of the runner
60 may be detected by the monitoring system, which is the mechanical basis used for crack monitoring
61 [9-12].

62

63 However, for Francis turbine, the modes at the working frequency area can be disk (band or
64 crown) dominated, particular for the pump turbine [14]. For the turbine researched now (see Figure
65 2), the modes at the working frequency area usually have high deformation both on the blades and
66 band[5, 6]. In some papers, they are called global modes [15] and it is even difficult to distinguish
67 they are band-dominated or blade-dominated. Unlike the discrete blades, the band is a continuous
68 structure. Sometimes, to do theoretical research on modal localization with consideration of the effect
69 of the disk, some researchers also discretized the continuous disk and simplified both the disk sectors
70 and blades into lump masses[8]. This procedure demonstrated that the disk-dominated modes and
71 blade-dominated modes are similar with only some parameter differences (see the Fig.11 in [8]).
72 Therefore, vibration localization can also occur for disk-dominated modes. Even so, the disk-
73 dominated modes or blade-dominated modes with high deformations on the disk are easy to have
74 high coupling stiffness between neighboring sectors and are difficult for strong localization to occur,
75 just as those shown in[13]. However, this may still depend on the geometry, and unlike the
76 centrifugal impeller, the band of the turbine shown in Figure 2 is more like a thin ring and the crown
77 usually has low deformation. The parameters of the blades are also different. Large uncertainties exist
78 as to whether strong vibration localization can occur in Francis turbine due to crack and how the
79 crack affects its modes. If strong vibration localization occurs, what of concern is whether it can cause
80 the natural frequencies to decrease drastically so that it could be detected by the monitoring system.
81 Another item of interest is whether under excitation forces, the crack can cause a vibration surge to
82 the runner which may also be captured by the monitoring system.

83

84

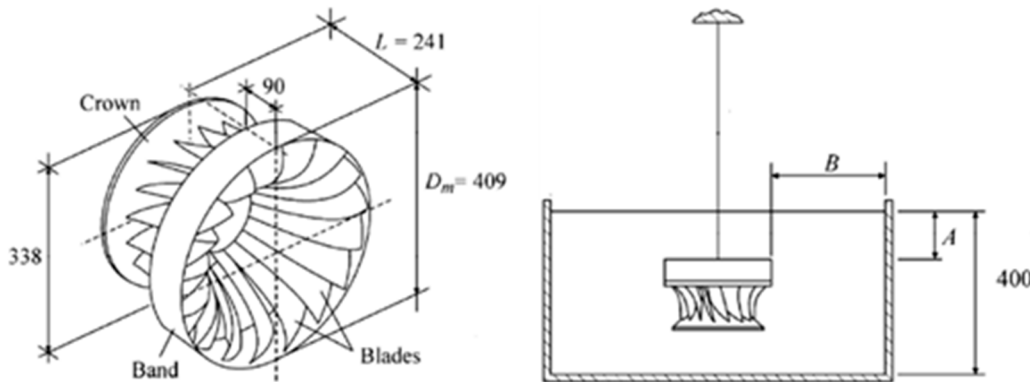


Figure 2. Geometry of the model and the view submerged in water [5]

85

86

87

88 In this paper, the dynamic behaviors of a Francis turbine runner mode (Figure 2) will be
 89 investigated numerically both in the air and in water. The numerical model geometry was built from
 90 the sketches of the experimental model used in [5] completed by CDIF-UPC and modified some parts
 91 through measurements. Modal localization theories will be used to explain the modal behavior
 92 changes due to crack. The forced response will be done to check the response changes due to crack.
 93 Finally, based on the above analysis, the crack monitoring challenge for Francis turbine will be
 94 analyzed, and the potential technologies to monitor the crack will also be introduced.

95 **2. Theoretical mode and theories**96 **2.1. Theoretical mode**

97 Theoretical modes usually are used to get general conclusions for one type of bladed-disk
 98 structures. In fact, it is sometimes hard to use one simplified theoretical mode to describe the whole
 99 vibration behaviors of one bladed-disk structure. Taking the widely used lumped parameter mode
 100 for example, it is usually hard to describe the unbalance problem due to the movements of real
 101 turbine blades because the roots of the lump masses are usually fixed. For the 1ND (Nodal Diameter)
 102 mode, due to the opposite vibration direction of two sides blades, the whole bladed-disk structure
 103 usually has a swing movement motion. This additional swing movement may increase the instability
 104 of the vibration. When there is a crack in the blade, the instability may have large effects on the
 105 vibration. Of course, for different ND modes, this additional movement would be different, and its
 106 effect would also be different. This is also true for the Francis turbine with so complicated geometry.
 107 However, here, we still try to simplify the Francis turbine runner to make the problem easier to
 108 understand.

109

110 When in the air, for each sector of Francis turbine, it consists one piece of crown, one blade and
 111 one piece of the band. If simplifying each of them to a lump mass using the method in [8], the system
 112 will be multi-coupled, which is very complicated. Little theories about the effect of crack on this
 113 system are available in the literature. For the low-order modes of the researched Francis turbine, the
 114 crown usually has relatively small modal displacement [6]. If neglecting the crown and seeing the
 115 connecting side of blades with it as fixed, the turbine can be simplified to the mode shown in Figure
 116 3(a). m_b and k_b are the blade (modal) mass and (modal) stiffness, respectively. The mass m_d
 117 simulates the effective mass of the corresponding section of the disk(band), and the stiffness k_d
 118 represents the stiffness of the rotor disk(band), whereas the massless spring stiffness k_c , provides
 119 disk coupling between neighboring sectors. This is a mono-coupled system, and its transfer matrix
 120 can be obtained using the method in [8]. However, the matrix is still complicated because of too many
 121 parameters.

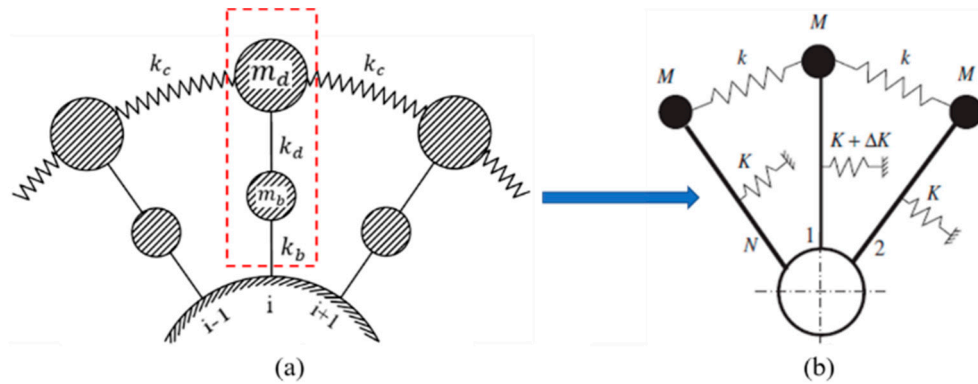


Figure 3. Theoretical modes

122

123

124

125 As aforementioned, this method indicates that the blades and band have similar modal
 126 behaviors with only some parameter differences. A simpler way is to simplify the band and single
 127 blade into one lump mass together as shown in Figure 3(b) and each lump mass contains two degrees
 128 of freedom, namely band and blade. Therefore, it will have blades dominated modes and band
 129 dominated modes. The modal behavior of this system with and without crack has been obtained in
 130 [16] and [17], respectively, which can be seen in section 2.2.

131 2.2. *Crack induced modal localization in mono-coupled system*

132 The whole system has N substructures and each substructure is simplified to a lump mass.
 133 Substructures with M mass and K stiffness are mono-coupled with massless springs, which stiffness
 134 is k. Substructure-1 is assumed to have a ΔK stiffness change.

135

136 For the tuned system, $\Delta K = 0$. The modal shapes can be divided into two categories:

137

$$138 \quad U_r^c = \{1, \cos \alpha_r, \dots, \cos(N-1)\alpha_r\}, \quad r = 1, \dots, \frac{N}{2} + 1 \quad (1)$$

139

$$140 \quad U_r^s = \{0, \sin \alpha_r, \dots, \sin(N-1)\alpha_r\}, \quad r = 2, \dots, \frac{N}{2} \quad (2)$$

141

142 where $\alpha_r = 2\pi(r-1)/N$. The corresponding eigenvalues are

143

$$144 \quad \omega_{0r}^2 = [1 + 2R^2(1 - \cos \alpha_r)] \cdot \omega_b^2 \quad (3)$$

145

146 Where $R^2 = k/K$ is the coupling effect and $\omega_b^2 = K/M$ is the natural frequency of the
 147 undamaged single substructure. The lower and upper limits of passband is

148

$$149 \quad \omega_L = \omega_b \quad \omega_U = \sqrt{1 + 4R^2}\omega_b \quad (4)$$

150

151 Note that except for k equals 1 or $N/2 + 1$, doublet eigenvalues occur, the corresponding
 152 eigenvectors being U_r^c and U_r^s (in fact, any linear combination of U_r^c and U_r^s is also an eigenvector).
 153 For periodic structures, they are usually called $(r-1)$ ND (node diameter) mode. For N odd, $N/2 +$
 154 1 is replaced by $(N+1)/2$ in (1-2), and there is only one simple eigenvalue for $r = 1$.

155

156 When substructure-1 has stiffness change, because of zero substructure-1 deformation of U_r^s ,
 157 these modes will not be affected by the mass or stiffness change. All the rest $N/2 + 1$ U_r^c modes will
 158 change and become chaos. Unlike the frequencies of other modes changing slightly, the 0 ND will
 159 quickly drop out of the pass-band and will be the only localized mode to the damaged sub-structure.
 160 For the localized mode, the damaged substructure(substructure-1) will have the largest deformation

161 and the deformation on other substructures will symmetrically attenuate around substructure-1. The
162 attenuation rate ξ will be:

163

164
$$\xi = \frac{q_1}{q_2} = \sqrt{1 + (\Delta f / 2R^2)^2} - |\Delta f / 2R^2| \quad (5)$$

165

166 Where the $\Delta f = \Delta K / K$ is the stiffness loss ratio of the damaged blade. Obviously, the attenuation
167 rate ξ is an odd function of $\Delta f / R^2$ ratio, the higher $\Delta f / R^2$, the higher severity of modal localization.
168 The frequency reduction ratio of the localized mode is

169

170
$$\lambda = 2R^2 \left(1 - \sqrt{1 + (\Delta f / 2R^2)^2} \right) \quad (6)$$

171

172 This procedure indicates that disk(band)-dominated modes also has modal localization to the
173 disk part if the corresponding blade has damage. However, for the real runner, the instability and
174 complicated blade-disk interaction [18] due to the unbalance problem aforementioned may bring
175 many differences.

176

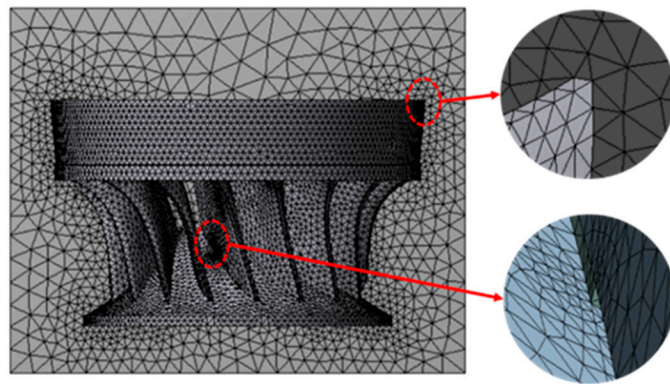
177 **3. Simulation setup**

178 The intact runner mode is a replica at a reduced scale of 1:10 of a Francis turbine runner with a
179 specific speed of 0.56. The model runner has 17 blades and a diameter of 409 mm. The shape of the
180 runner with the main dimensions is shown in Figure 2. The material used is a bronze alloy whose
181 properties are given by Table 1.

182

183 First, the intact runner mode will be validated by comparing its modal analysis results in air and
184 water with the experimental results in [5]. Ansys 16.2 was used to handle all the simulations in this
185 paper, and the acoustic FSI technology is used to simulate the added mass effect from surrounding
186 water [6]. The material property of the acoustic body can be seen in Table 2. When the runner is
187 submerged in water, common nodes technology is used at all the FSI interfaces, and the Asymmetric
188 solver is used in the simulation. The distances A and B shown in Figure 1 are 100mm and 45mm,
189 respectively. The upper surface of the water domain was set as zero-pressure surface and all other
190 outside boundaries of water domain were set as rigid walls. The mesh sensitivity is strictly checked,
191 and when the runner is submerged in water, approximately 192,391 tetrahedral elements are used.
192 Because the damping has little effects on the modal behavior of the structure, the structure damping
193 and the viscosity of the acoustic body are neglected [5, 6]. The comparison between the numerical and
194 experimental results in [5] can be seen in Table 3. As seen, good agreement has been obtained.

195



196

197

198

199

Figure 4. View of the mesh

200 Based on the validation of the intact runner, a crack is created at the intersection line between
 201 one blade and the crown from inside to outside, a location that has been shown to be prone to the
 202 occurrence of cracks in the Francis turbine [2]. The crack is represented as a narrow gap, and this is a
 203 linear method that has been used in much of the literature [17]. The total length of the intersection
 204 line is approximately 120 mm and the crack length in this paper will vary from 0 mm to 100 mm. The
 205 mesh density at the crack tip has been especially increased as shown in Figure 4. When submerged
 206 in water, the water at the crack clearance is neglected. The effects of the crack on the dynamic
 207 behaviors of the runner will be investigated.

208

209

Table 1. Properties of the runner material

Properties	Young's modulus	Density	Poisson's ratio
Value	110 GPa	8300 kg/m ³	0.34

210

211

Table 2. Properties of the acoustic body

Properties	Sonic speed	Density
Value	1483 m/s	1000 kg/m ³

212

213

Table 3. Results of the experimental and numerical modal analysis

214 SIM-AIR: Simulation in air (unit: Hz) EXP-AIR: Experiment in air SIM-RATIO: SIM-WATER/SIM-AIR

	SIM-AIR	EXP-AIR	SIM-WATER	EXP-WATER	SIM-RATIO	EXP-RATIO
2ND	357.00	373.51	275.89	279.50	0.773	0.748
0ND	408.38	417.50	374.73	370.50	0.907	0.887
3ND	475.98	487.53	338.26	331.25	0.711	0.679
4ND	563.50	573.75	369.36	359.00	0.656	0.626
1ND	606.20	616.75	489.62	481.50	0.808	0.781
5ND	634.85	649.75	391.65	400.00	0.617	0.616

215

216 4. RESULTS AND DISCUSSION

217 4.1. Modal behavior

218 4.1.1 Natural frequencies and modal shapes

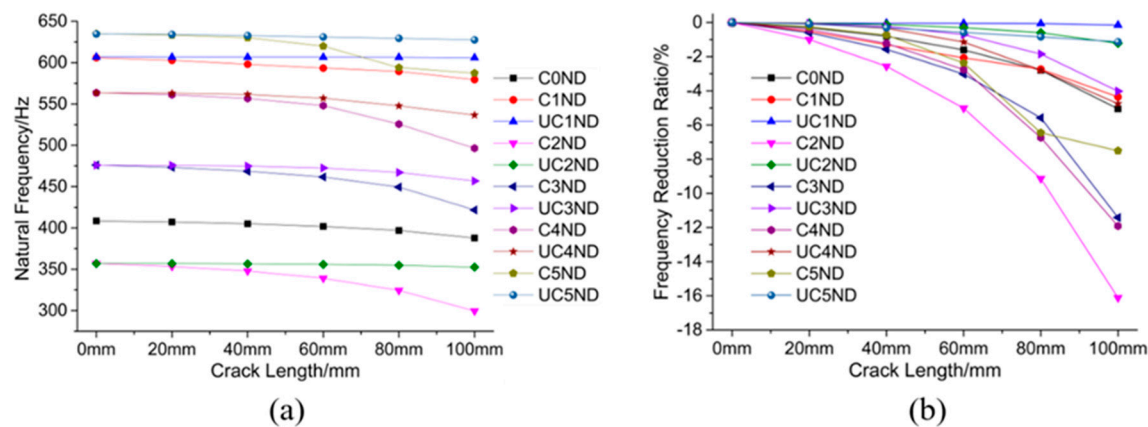
219 The modal shapes without a crack, with a 60 mm crack and with a 100 mm crack in the air and
 220 water can be seen in Table 4 and Table 5, respectively. For each simulation case, the modal
 221 displacement is divided into nine levels from high to low so that they can be compared together. The
 222 changes in both the natural frequency and the frequency-reduction ratios with the crack length in air
 223 and water can be seen in Figure 5 and Figure 6, respectively.

224

225 Obviously, the modal shapes are different in the air and water for the same ND modes with the
 226 same crack length, which has also been shown in [6]. This may be mainly because the blades and the
 227 band suffer from different added mass factors [5] in water for such structures with the different parts
 228 separated enough to have their own dominant modes. Due to the modal shape change from air to
 229 water, the frequency changes with increasing crack length in air and water will also be very different,
 230 as shown in Figure 5 and Figure 6. Therefore, the Francis turbine in water can be seen as a new bladed-
 231 disk structure with the band, crown and blades having different densities. Of course, due to the close
 232 distance between the blades, each may affect the vibration of nearby blades through hydraulic
 233 force[19], which may cause the system to be multi-coupled[8]. However, for the researched modes,
 234 this coupling stiffness from hydraulic force ought to be very small compared with the coupling
 235 stiffness from band deformation and thus its effect may be very limited. Therefore, the effect of a
 236 crack on the modal behavior in air and water ought to show many similarities, which can be seen in
 237 the following analysis.

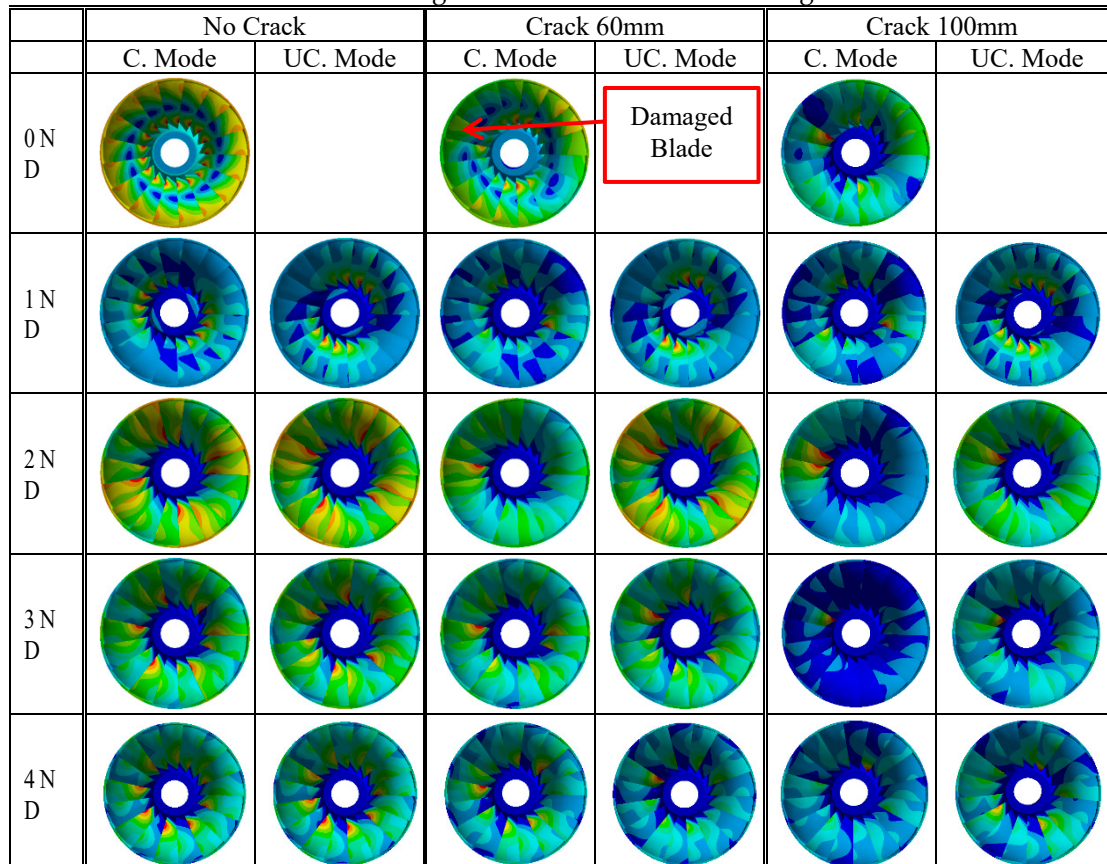
238

239 From the modal shapes and natural frequencies, the singlet 0ND and one of the doublet modes
 240 of each ND will change relatively more, while the remaining one of the doublet mode of each ND
 241 will change relatively less. Generally, for actual turbines, there are no substructures that are without
 242 any deformation. Therefore, there are no modes that are completely unaffected by the crack.
 243 However, one of the doublet modes of each ND continues to change relatively more and the other
 244 one changes much less, which means the principle of the change in modes due to the crack is still in
 245 accordance with the theoretical analysis. In the following parts, the modes changing more are referred
 246 to as changed modes, and modes changing less are referred to as unchanged modes.
 247



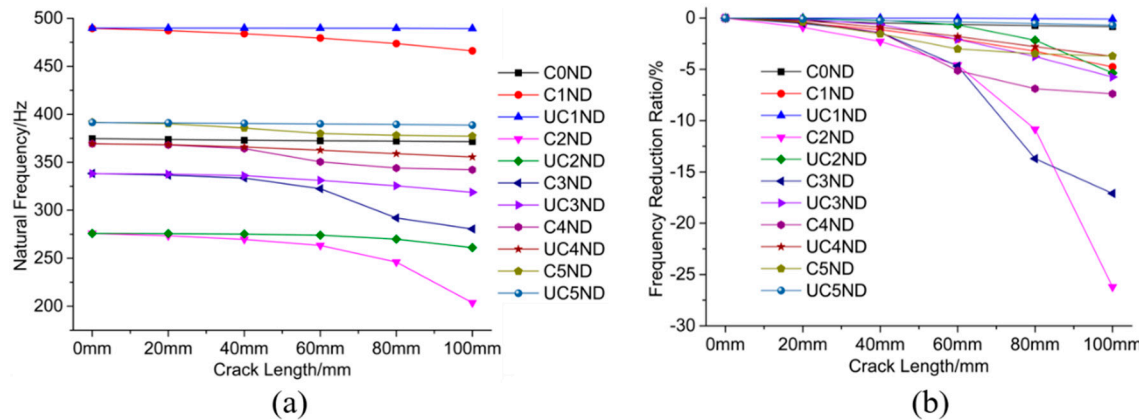
248
 249
 250
 251
 252 Figure 5. Natural frequency changes and change ratios in air

Table 4. Modal shape changes in air
 C.Mode: changed mode UC. Mode: unchanged mode

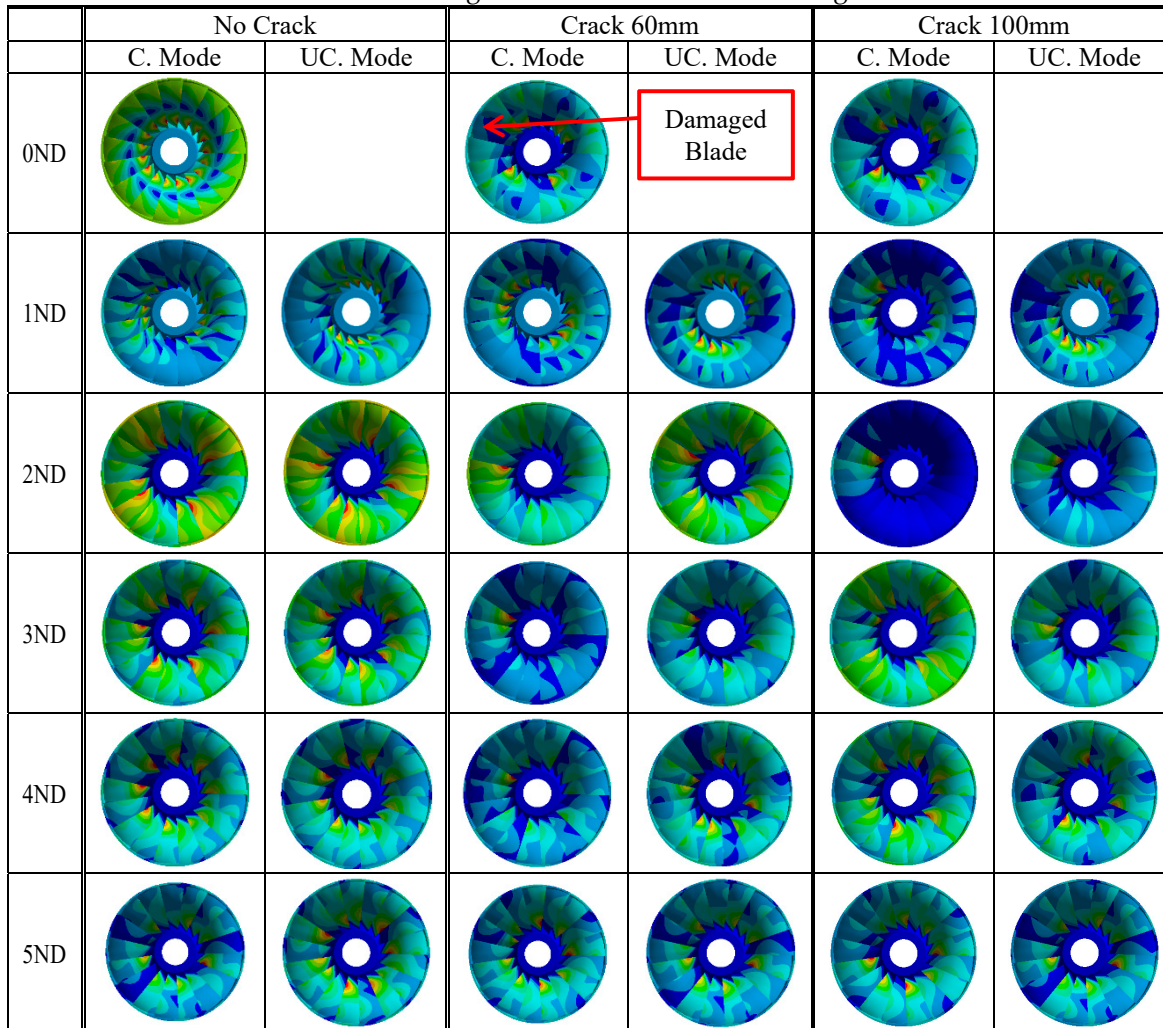


253
 254 When comparing the modal shape changes of the changed and unchanged doublet modes of
 255 each ND with the change in crack length, for most ND modes the changed mode usually originates

256 from the one with low deformation on the damaged blade, and the damaged blade is close to the
 257 zero-displacement node. In contrast, for the 1ND and 8ND modes, which have nearly zero
 258 deformation blades, the changed mode usually originates from the one with high deformation on the
 259 damaged blade, and the damaged blade is far from the zero-displacement node.



260

261 Figure 6. Natural frequency changes and change ratios in water
 262263
 264Table 5. Modal shape changes in water
 C.Mode: changed mode UC. Mode: unchanged mode

265

266 The modal shape changes with the increase in crack length are not that regular, which may be
267 because of the vibration instability mentioned above under the complicated high-intensity interaction
268 between the blades and disk. Due to the differences in vibration motion of the different ND modes,
269 the changes can vary significantly. For all the unchanged modes, the modal shapes may also become
270 distorted to some extent with an increase in crack length. Apart from the unchanged 1ND, which has
271 low deformation at the damaged blade, the damaged blade is prone to having a large deformation at
272 the beginning part of the crack. This high deformation can cause the energy to concentrate at that
273 part, which will induce deformation degeneration at the band and other blades.

274

275 For the changed modes, the modal shape changes are even more irregular than those of the
276 unchanged modes. Sometimes, under certain crack lengths, the highest deformation may appear at
277 blades near the damaged blade, but when the crack length is very large, it will finally transmit to the
278 damaged blade, like the changed 2ND and 3ND mode in air. Obviously, both in the air and in water,
279 the changed 2ND mode has a high deformation concentration in the band near the damaged blade.
280 This is the only mode that has a deformation concentration on the band near the damaged blade.
281 Therefore, it ought to be the localized mode. The concentration usually is at the band piece next to
282 the damaged blade sector when the crack is short, but it will finally transmit to the damaged blade
283 sector and the localization becomes very strong when the crack is long.

284

285 The 3ND in the air with a crack length of 100 mm is a special case, which has a high deformation
286 concentration at the damaged blade with strong deformation degeneration at the band and other
287 blades. This mode may be not the localized mode because the band deformation has no concentration
288 near the damaged blade. The origin of this mode may be the vibration instability mentioned earlier.
289 The 3ND mode in water presents an interesting situation. When the crack is not too long, e.g., 60 mm,
290 this mode shows a high deformation concentration on the damaged blade with deformation
291 degeneration on the band. However, when the crack is long, e.g., 100 mm, the modal shape of the
292 changed 3ND becomes similar to that of the 2ND. From Figure 5, the natural frequency of the changed
293 3ND with a 100 mm crack is close to that of the 2ND mode. This means that when the changed modes
294 are close to other modes with the reduction of frequencies, the modal shapes will become similar
295 with the modes that they will pass.

296

297 For the unchanged modes, the frequency reduction ratios are usually lower than 5% when the
298 crack length is 100 mm. For some modes, such as the unchanged 1ND, the frequency reduction ratio
299 can be as low as 0.1%. For the changed modes, the localized mode usually has a relatively high-
300 frequency reduction ratio. When the crack length is 100 mm, the frequency reduction ratios of the
301 localized 2ND can be as high as 16% in air and 26.5% in water. Though the changed 3ND mode in air
302 has a high deformation concentration on the damaged blade when the crack length is 100 mm, its
303 frequency reduction ratio is much lower than the localized 2ND. This may have a relationship with
304 the damaged blade deformation, which means that for the changed 3ND mode, the deformation
305 concentrates on the beginning part of the crack in the damaged blade and this modal shape of the
306 damaged blade may not cause a high stiffness reduction ratio. However, when in water with a crack
307 length of 60 mm, the frequency reduction ratio of the 3ND mode is higher than that of the localized
308 2ND mode. In addition to the damaged blade having a modal shape with the highest deformation at
309 its middle part, the deformation concentration degree may also contribute to it, which means the
310 changed 3ND has a higher deformation concentration degree than the localized 2ND mode in water.

311

312 As mentioned earlier, when the changed modes are close to other modes with the reduction of
313 frequencies, the modal shapes will become similar with the modes that they will pass. This
314 phenomenon may have large effects on the frequency reduction ratios of the changed modes. In
315 water, this phenomenon can be more significant than in air because the frequencies of different modes
316 are closer. For the changed 3ND, 4ND and 5ND modes in water as well as the changed 5ND mode in
317 air, when this phenomenon occurs with an increase in crack length, the frequency reduction is greatly

318 decreased. Overall, the natural frequency changes for all ND modes are limited. This is due to two
 319 main reasons. On the one hand, though the band is like a thin ring, the couplings between
 320 neighboring sectors are still very high. On the other hand, the blades are firmly constrained by the
 321 band and the crown, which may reduce the stiffness reduction ratio. For different modes, the
 322 frequency reduction ratios can vary significantly.

323

324 In reality, the runner is connected to the shaft. By assuming that the shaft is nearly rigid, a fixed
 325 support is given to the top surface of the crown, as shown in Fig. 9(support A), and the modal shapes
 326 under the fixed support in the air are shown in Table 6. Due to the fixed support, the 0ND, 1ND and
 327 2ND modes were reduced from 408.38 Hz, 605.84 Hz and 356.95 Hz to 256.43 Hz, 301.43 Hz and
 328 369.27 Hz, respectively. This means that these three modes have more deformations on the crown
 329 part, particular the 0ND and 1ND. There are also large changes in the modal shapes of 0ND and 1ND.
 330 The natural frequencies of the higher ND modes are almost unaffected by the fixed support.
 331 Obviously, the 0ND mode quickly becomes localized with the increase in crack length. The
 332 interesting thing about the 1ND is that it also shows some localization, even though the degree of
 333 localization is much less than 0ND. The 2ND mode no longer has localization. The 3ND mode still
 334 shows a strong deformation concentration at the damaged blade when the crack is 100 mm. From the
 335 above analysis, the mode with the lowest natural frequency is most prone to localize. This may have
 336 a relationship with the blade-disk interaction property and the mode with the lowest frequency is
 337 just at its veering point [18]. That 1ND shows some localization may be because of its relatively low
 338 frequency and the strong instability of its vibration. When there is no fixed support at the crown, the
 339 1ND mode is at high-frequency area, and no localization occurs to it. Considering the low degree of
 340 localization of 1ND, it may be considered that there is still only one localized mode.

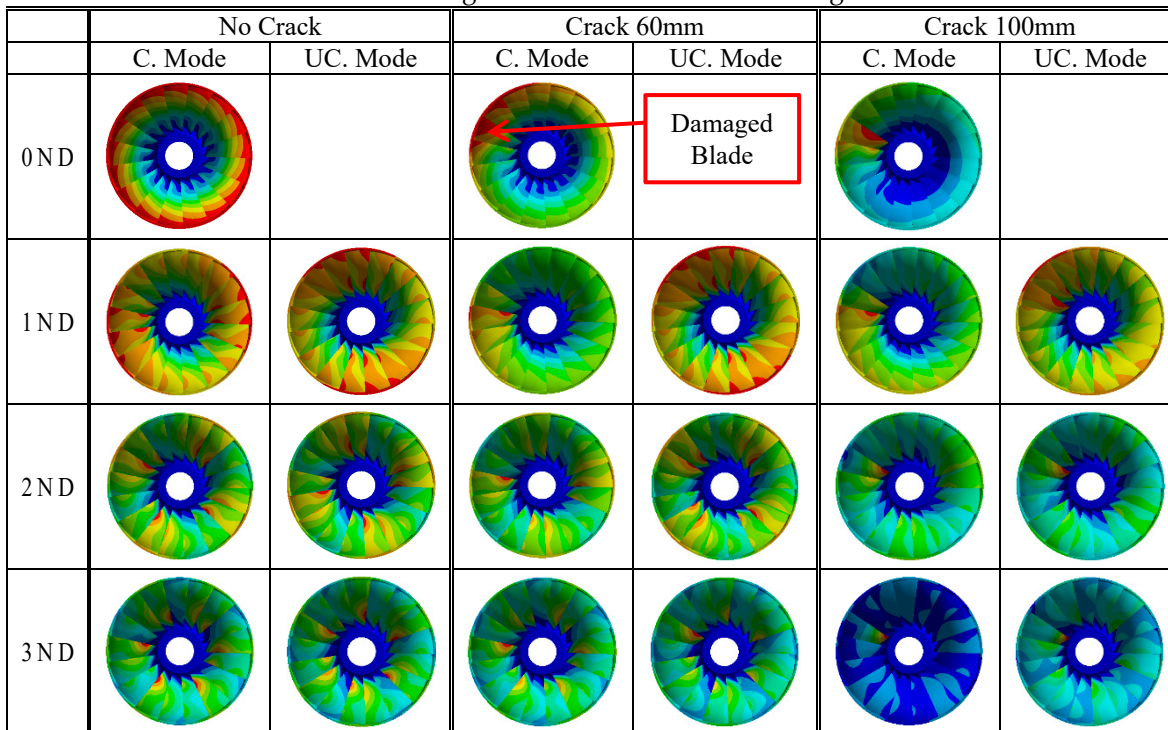
341

342

343

Table 6. Modal shape changes in air with fixed support

C.Mode: changed mode UC. Mode: unchanged mode

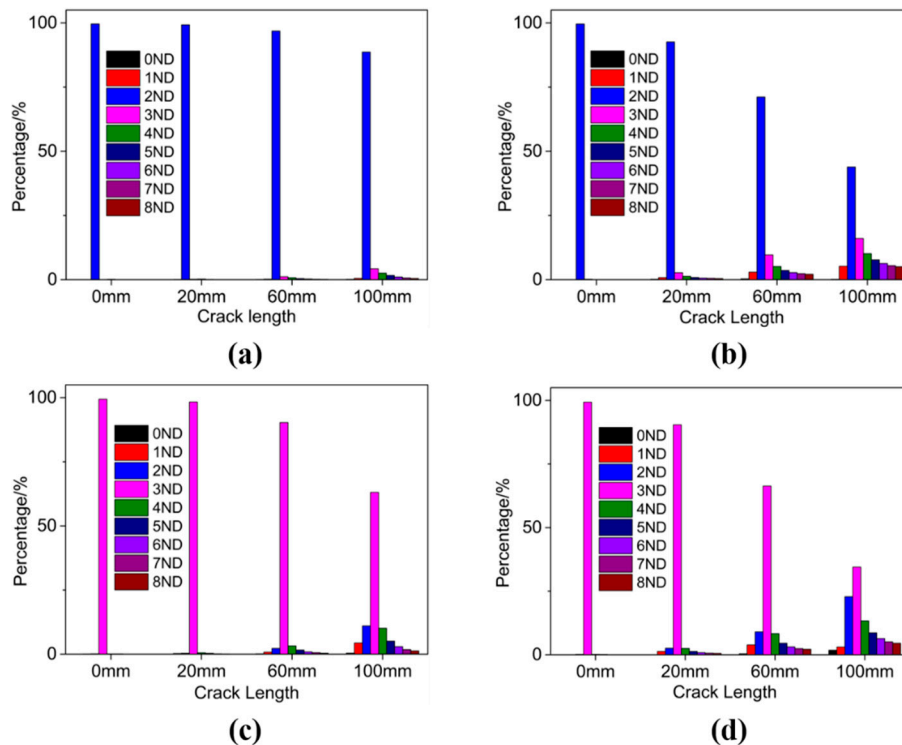


344

345 4.1.2 FFT of modal shapes and the localization factor

346 The modal shape change due to a crack can also be described using a Fast Fourier Transform
 347 (FFT) of the modal shape. The first step of this procedure is to choose the sample point to represent
 348 the modal shape change. First, the sample point is chosen as the intersection point of the trailing edge

349 and the band for each blade. Therefore, 17 sample points were obtained, and the modal displacement
 350 variation of these 17 points for each mode was used for FFT. The FFT results of the changed 2ND,
 351 unchanged 2ND, unchanged 3ND and changed 3ND in air for crack lengths of 0 mm, 60 mm and 100
 352 mm are shown in Figure 7(a), (b), (c) and (d), respectively. Each modal shape can be seen to be
 353 synthesized by different ND harmonic waveforms with different magnitudes. For each ND, its value
 354 was plotted by the percentage of its magnitude to the sum of the magnitudes of all ND waveforms.
 355



356
 357 Figure 7. FFT results to the modal shapes
 358

359 Without a crack, each modal shape clearly contains only one waveform. With the increase in
 360 crack length, the percentage value of this original waveform will continue to decrease and other ND
 361 waveforms will appear with increased percentage value. For the unchanged modes, the decrease in
 362 the original ND waveform and the increase other ND waveforms are very insignificant, while for the
 363 changed modes, they are much more significant, particular for the localized mode and the mode with
 364 strong deformation concentration to the damaged blade (like the changed 3ND in Figure 7(d)). The
 365 values of the new appearing ND waveforms usually decrease with their separation from the original
 366 ND waveform.
 367

368 For a Francis turbine, the excitation from the hydraulic force is due to the rotor-stator interaction
 369 and the excitation is order excitation. To make the runner resonant, both the frequency and the ND
 370 of the excitation should be in accordance with the runner mode. This is to say that only the mode
 371 with the same ND can extract energy from the excitation force. When a crack is present, other ND
 372 waveforms start to appear. This means that the mode now can not only be excited by the original ND
 373 excitation but also be excited by other ND excitations. With an increase in the crack length, the
 374 decrease in the original ND percentage value means the ability to extract energy from the
 375 corresponding ND excitation decreases and the increase in the other ND percentage values means
 376 the ability to extract energy from the corresponding ND excitation increases[20]. However, the FFT
 377 value change may quite depend on the sample points positions because with the crack, the
 378 deformations on the blades, particular the damaged blade, become very ununiform. With other
 379 groups of sample points, the FFT results may vary a lot and become not that regular. However, using

380 those sample points may be not appropriate because of the locally unregular deformation change on
 381 the damaged blade and it may be better to use the sample points on the band.

382

383 The maximum response under order excitation not only depends on the FFT value change but
 384 also depends on the Localization Factor(LF) [21] change. The LF is defined as:

385

$$386 \quad LF = \frac{U_{1\ max} - U_{0\ max}}{U_{0\ max}} \times 100\% \quad (7)$$

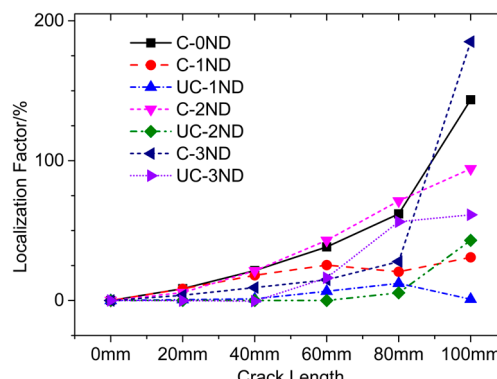
387

388 Where $U_{0\ max}$ is the maximum modal displacement of one mode without crack and $U_{1\ max}$ is the
 389 maximum modal displacement of the mode with crack. The LF describes the frequency response
 390 function(FRF) change due to crack under point excitation for one mode. Of course, the damping is
 391 not considered in the modal analysis and this may have some effects on the LF values. With damage,
 392 the deformation will have concentrations, which will induce the increase of the modal displacement.
 393 When the frequency change due to crack is not that too large, the deformation concentration will
 394 increase the LF value. From Figure 8, for most modes, the LF will increase with the crack length
 395 increase. The increases for changed modes are much more significant than the unchanged modes due
 396 to higher deformation concentrations. When the crack length is high, the modal shape changes may
 397 be very complicated and the LF values may decrease, like the unchanged 1ND mode from crack
 398 80mm to 100mm.

399

400 However, for an actual Francis turbine, the excitation is order excitation and the excitation
 401 energy depends on the FFT value in Figure 7. If the FFT value increases, and the LF value increases
 402 with increasing crack length, the maximum deformation change of the forced response will increase.
 403 If the FFT value decreases and the LF value increases with increasing crack length, the maximum
 404 deformation change of the forced response will depend on the change rates of the two values.

405



406
 407 Figure 8. LF value changes with the crack length
 408

409 4.2. Forced response

410 The forced response was carried out through harmonic response analysis. The top face of the
 411 crown was fixed, and the amplitude of dynamic pressure was 0.01Mpa (seen in Figure 9). Here we
 412 use the constant pressure to research the property change of the runner, which is a common method
 413 used in[10, 12, 13, 17]. In [17], the analytic method was used to analyze the forced response of the
 414 localized 0ND in mono-coupled lumped parameter system. However, the analysis on the forced
 415 responses of other nonlocalized modes was very little. Furthermore, the analytical method is very
 416 complicated and not very intuitionistic. For real Francis turbine, the responses may also be not as
 417 regular as those in lumped parameter system. In this paper, the forced responses will be analyzed
 418 based on the modal shape FFT results and LF value changes, which is more intuitionistic and easier
 419 to understand. Dynamic pressures were applied to the pressure side of each blade. To get certain ND

420 order excitation, there were corresponding phase changes between neighboring blades. Because in
 421 water, the dynamic behaviors of the runner have no essential differences with those in the air, the
 422 analysis was only done for the runner in the air. The forced responses under 3ND excitation is shown
 423 in Figure 10.

424

425 The experimental damping ratio of 3ND mode 0.0068 was implemented because the 3ND mode
 426 has the highest response and damping ratio has larger effects on the higher response. The FFT and
 427 LF values obtained above are based on the modal analysis without fixed support on the crown.
 428 However, for 3ND mode, the effects of fixed support are very little. Therefore, they are still used to
 429 explain the forced response changes.

430



A:Fixed Support
 Others: Dynamic Pressures

Figure 9. Boundary conditions and loads

431

432

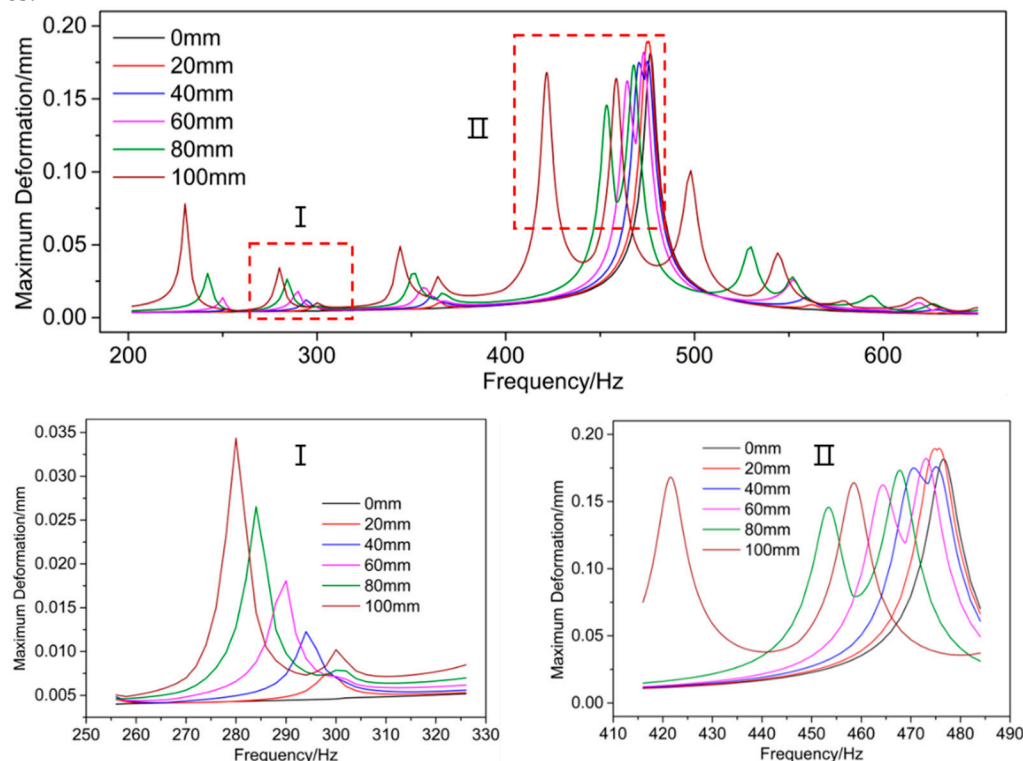
433

434 For 3ND excitation, the unchanged 3ND mode and the changed 3ND mode certainly have the
 435 highest responses (shown in II of Figure 10). For the undamaged runner, there is only one peak due
 436 to the same natural frequencies of the changed and unchanged 3ND modes. With the increase of the
 437 crack length, these two modes become separated, and two peaks appear. The first peak corresponds
 438 to the changed mode and the second peak corresponds to the unchanged mode. For the changed 3ND
 439 mode, the response at crack 20mm is the highest, which means the increase of the LF value is faster
 440 than the decrease of 3ND FFT percentage value from 0mm to 20mm. From 20mm to 80mm, the
 441 response decreases gradually, which is because the 3ND FFT value of this mode decreases fast, while
 442 the LF value increases moderately during the progress. From 80mm to 100mm, there is a drastic
 443 response increase, which is due to the drastic LF value increase as shown in Figure 8. For the
 444 unchanged 3ND mode, the response with 20 mm long crack is also highest. When with 20mm crack,
 445 the peaks of changed and unchanged modes are very close, and they may affect each other's response
 446 to some extent. From 20 mm to 100 mm, the response change is not that regular and reaches its
 447 minimum at 100mm. From Figure 8, the LF value of the unchanged 3ND mode increases drastically
 448 from 20mm to 80mm, which may be the reason why the response at 60mm is higher than that at
 449 40mm. At 40mm, the peaks of changed and unchanged modes are approximately the same, this is
 450 because the LF value of the changed mode is a little higher while the FFT value is a little lower compared
 451 with those of the unchanged mode. At 60mm or 80mm, the peak of the unchanged mode is much higher
 452 than that of the changed mode due to the both higher LF and FFT values. At 100mm, the levels of
 453 these two peaks are close again.

454

455 For the 1ND mode without crack under 3ND excitation, the response (seen in I of Figure 10)
 456 certainly is very low. With the increase of crack length, the response of the changed 1ND mode
 457 increases drastically. This is because both the 3ND FFT value and the LF value of 1ND mode increase
 458 with the crack length. The response of unchanged 1ND under 3ND excitation is much lower, and
 459 only a little peak appears when the crack is 100mm. The response changes of 0ND, 2ND and 4ND
 460 modes are similar with that of 1ND. However, the responses of 0ND and 4ND at crack 100mm are
 461 much higher than that of 2ND. This is because of the great increases of the LF values due to the high

462 deformation concentrations of these two modes (see Figure 8). When the crack length is not that high,
 463 like less than 60mm, all these peak levels are still limited due to the moderate increases of the LF and
 464 FFT values.



465
 466 Figure 10. Forced responses under 3ND excitation
 467

468 Overall, both for the changed and unchanged modes under the same ND excitation, with the
 469 increase of crack length, the responses usually increase first and then decrease, even though the
 470 increase and decrease progress are not monotone. This change progress is similar to the force
 471 response changes of the localized mode in lumped parameter system with crack severity[17]. Except
 472 the localized 0ND, the forced responses of other modes decrease with apart from 3ND. This is because
 473 the FFT percentage values of new appearing ND waveforms usually decrease with apart from the
 474 original ND waveform as aforementioned. This point is very similar to the forced response changes
 475 of localized 0ND with excitation order in lumped parameter system, which has a decreased response
 476 with increase the ND of excitation (apart from 0ND)[17]. Therefore, the forced responses of localized
 477 and nonlocalized modes indeed share many similarities. From the response peak changes of all the
 478 modes, the method that using the FFT and LF value changes to explain the response changes is
 479 basically appropriate.

480

481 For the researched Francis turbine, when the crack length is high, the frequency reduction ratios
 482 can be higher than 20% (mainly referring to the localized mode or the modes with strong deformation
 483 concentrations on the damaged blade). However, when the crack is not that large, the natural
 484 frequency reduction ratios are usually less than 10%. For this type of machine, there is usually a safety
 485 margin in the operation to avoid resonance, such as 20% of the natural frequency (corresponding to
 486 the ND of the RSI excitation). Therefore, it is very difficult for the natural frequency to fall to the
 487 operating area to be excited and to be detected by the current monitoring system.

488

489 Though the responses of other modes (not corresponding to the ND of the RSI excitation)
 490 increase with crack length and these modes are in the operating region, when the crack length is not
 491 high enough (often less than 60 mm), the response increases are still limited. Because the peak
 492 increases due to a crack are limited, they might very easily be confused with a load change, and it
 493 can be difficult to activate the vibration alarm of the turbine. Another very important thing is that the

494 current monitoring system is usually at the bearing of the turbine. The vibration of runner must be
495 transmitted to the bearing through the shaft, and the vibrations are also easily confused with the
496 bearing effect. The response used in this paper is the maximum response of the runner, which is also
497 used in many other papers[10, 12, 13]. However, due to the vibration being transmitting to the
498 monitoring system, the equivalence between the maximum local response increase due to a crack and
499 the vibration increase captured by the monitoring system is still doubtful.

500

501 For the Francis turbine shown in Figure 1, its modal behavior is still not that clear and the crown
502 may have a high deformation. Under this situation, it will be multi-coupled, and more than one
503 localized mode may appear. Doublet modes can still be divided into changed modes and unchanged
504 modes, just as for the impeller in[13]. However, the higher deformation at the crown will greatly
505 increase the coupling stiffness, which will cause the natural frequency reduction ratios and the
506 response changes to be much lower (5-6) [17]. This will greatly increase the monitoring difficulty and
507 may be the reason why a so large crack was not detected by the monitoring system.

508

509 The value of the current research is twofold. First, it clarifies the effect of a crack on the dynamic
510 behavior of a Francis turbine from the viewpoint of vibration localization and the challenge of crack
511 monitoring. Second, this research can provide some references for more advanced crack-monitoring
512 technologies. Though the frequency deviations are low, they maybe can be captured by more
513 advanced monitoring technologies. David Valentín et al [15]has done some researches on the
514 feasibility of detecting natural frequencies of hydraulic turbines while in operation using strain
515 gauges. Therefore, the natural frequency changes of the runner in operation maybe can be detected
516 more accurately and through these changes, the crack maybe can be detected much earlier. Of course,
517 the phenomenon that the modal shape of the changed mode may become similar with another mode
518 when their frequencies are close as aforementioned should be paid special attention to during the
519 progress, because when the natural frequencies and modal shapes are similar, they are very easy to
520 be confused, which may greatly increase the monitoring difficulty. It seems that the lowest frequency
521 mode is ideal for monitoring because it is usually the localized mode which has highest frequency
522 reduction ratio and is not affected by the above-mentioned phenomenon. However, due to the lowest
523 frequency, its frequency value change may be also very low, which makes it easy to be confused by
524 the monitoring error. While the higher frequency modes have advantages in this aspect. R.A. Saeed
525 et al [22] has done some works on the crack monitoring using artificial intelligence technology based
526 on the maximum forced responses of the runner. However, the maximum response may be difficult
527 to obtain in real case. Anyway, this technology has developed very fast during the past few years and
528 shows great potential[23]. Due to the low frequency and response changes as shown in the above
529 analysis, this technology combined with the on-runner measurements is specially recommended for
530 further research in the future.

531

532 CONCLUSIONS

533 The modal behaviors and forced responses of a Francis runner model with a crack were studied
534 numerically in this paper and the crack-induced vibration localization theory was used to explain the
535 dynamic behavior changes. Some main conclusions are as follows:

536

537 For the studied Francis runner model, the crown has a low modal displacement. Therefore, it
538 almost can be seen as a mono-coupled system. There is usually only one localized mode and when
539 the crack length is high, strong localization can occur. The mode with the lowest natural frequency is
540 easiest to localize. The singlet modes and one of the doublet modes for each ND will change much
541 more, and the remaining doublet modes will change much less. All these matches the theories well.
542 However, perhaps due to the vibration instability, the modal shape changes are not that regular, and
543 some non-localized modes may show strong deformation concentrations on the damaged blade. The
544 frequency reduction ratios of the changed modes are relatively higher than those of unchanged

545 modes. The localized mode or the modes with strong deformation concentrations on the damaged
546 blade usually have the highest natural frequency reduction ratios. The modal shapes and frequency
547 reduction ratios in water are different from those in the air because the band and blades suffer from
548 different added mass factors in water. The modal shape of a changed mode may become similar with
549 another mode when their frequencies are close. The FFT percentage value of the original ND for one
550 mode usually decreases with the increase in crack length, while the FFT percentage values of other
551 NDs usually increases with the increase in crack length. The LF values usually increase with an
552 increase in crack length and the LF value changes of the changed modes are usually higher than those
553 of the corresponding ND unchanged modes.

554

555 For one mode under the same ND excitation with constant pressure, the forced response usually
556 first increases and then decreases with the increase in crack length, but the progress may not be
557 monotone. The response of one mode under other ND excitations will increase gradually and the
558 response can be very high when the crack is long. The method that using the FFT and LF value
559 changes to explain the response changes is basically appropriate.

560

561 Though the band is similar to a thin ring, it is still very stable. Therefore, the coupling stiffness
562 is very high, which makes the natural frequency reduction ratios less than 10%, and the forced
563 response changes are limited when the crack is not long enough. These are the reasons why the crack
564 is difficult to be monitored in this type of runner. The research in this paper can provide some
565 references for more advanced monitoring technologies.

566

567 **Author Contributions:** Ming Zhang did the simulation and wrote the paper; Xingfang Zhang
568 contributed jointly by supervising the overall work and overall structure of the paper; Weiqiang Zhao
569 helped to improve the quality of some pictures and the language of the paper.

570

571 **Acknowledgments:** The present research work was financially supported by China Scholarship
572 Council.

573

574 **Conflicts of Interest:** The authors declare no conflict of interest.

575

576 Nomenclature

577	FFT	Fast Fourier Transform	577	LF	Localization Factor
578	m_b	Blade modal mass	578	m_d	Disk modal mass
579	k_b	Blade modal stiffness	579	k_d	Disk modal stiffness
580	k_c	Coupling stiffness	580	N	Number of blades
581	M	Mass of the substructure	581	K	Stiffness of the substructure
582	ΔK	Stiffness change of the substructure	582	U_r^c	Cosine category of modal shapes
583	U_r^s	Sine category of modal shapes	583	ξ	Attenuation rate
584	r	Engeon order	584	Δf	Stiffness loss ratio
585	ND	Nodal Diameter	585	R	Coupling stiffness
586	ω_L	Lower limit of the pass-band	586	ω_U	Upper limit of the pass-band
587	q	Modal displacement of the substructure			
588	α_r ,	Phase change of neighboring substructures			
589	ω_{0r}	Natural frequency of the undamaged ($r - 1$)ND mode			
590	ω_b	Natural frequency of the undamaged substructure			
591	λ	Frequency reduction ratio of the localized mode			
592	$U_{0\ max}$	maximum modal displacement of one mode without crack			
593	$U_{1\ max}$	maximum modal displacement of one mode without crack			
594					

595 **References**

596 1. Liu, X., Y. Luo, and Z. Wang, A review on fatigue damage mechanism in hydro turbines.
597 Renewable and Sustainable Energy Reviews, 2016. 54: p. 1-14.

598 2. Frunzăverde, D., et al., Failure analysis of a Francis turbine runner. IOP Conference Series: Earth
599 and Environmental Science, 2010. 12.

600 3. Flores, M., G. Urquiza, and J.M. Rodríguez, A Fatigue Analysis of a Hydraulic Francis Turbine
601 Runner. World Journal of Mechanics, 2012. 02(01): p. 28-34.

602 4. Egusquiza, E., et al., Condition monitoring of pump-turbines. New challenges. Measurement,
603 2015. 67: p. 151-163.

604 5. Rodriguez, C.G., et al., Experimental investigation of added mass effects on a Francis turbine
605 runner in still water. Journal of Fluids and Structures, 2006. 22(5): p. 699-712.

606 6. Liang, Q.W., et al., Numerical simulation of fluid added mass effect on a francis turbine runner.
607 Computers & Fluids, 2007. 36(6): p. 1106-1118.

608 7. Cai C W, Cheung Y K, Chan H C. Mode localization phenomena in nearly periodic systems[J].
609 Journal of applied mechanics, 1995, 62(1): 141-149.

610 8. Ottarsson G, Pierre C. Vibration localization in mono-and bi-coupled bladed disks-a transfer
611 matrix approach[C]//34th Structures, Structural Dynamics and Materials Conference. 1993: 1492.

612 9. Saito A, Castanier M P, Pierre C. Effects of a cracked blade on mistuned turbine engine rotor
613 vibration[J]. Journal of vibration and acoustics, 2009, 131(6): 061006.

614 10. Kuang J H, Huang B W. The effect of blade crack on mode localization in rotating bladed disks[J].
615 Journal of sound and vibration, 1999, 227(1): 85-103.

616 11. Jung C, Saito A, Epureanu B I. Detection of cracks in mistuned bladed disks using reduced-order
617 models and vibration data[J]. Journal of Vibration and Acoustics, 2012, 134(6): 061010.

618 12. D'Souza, K., A. Saito, and B.I. Epureanu, Reduced-Order Modeling for Nonlinear Analysis of
619 Cracked Mistuned Multistage Bladed-Disk Systems. AIAA Journal, 2012. 50(2): p. 304-312.

620 13. Wang, S., et al., Reduced-order modeling for mistuned centrifugal impellers with crack
621 damages. Journal of Sound and Vibration, 2014. 333(25): p. 6979-6995.

622 14. Valero, C., et al., Modal behavior of a reduced scale pump turbine impeller. Part II: Numerical
623 simulation. IOP Conference Series: Earth and Environmental Science, 2010. 12.

624 15. Valentin, D., et al., Feasibility of Detecting Natural Frequencies of Hydraulic Turbines While in
625 Operation, Using Strain Gauges. Sensors (Basel), 2018. 18(1).

626 16. Wei S T, Pierre C. Localization phenomena in mistuned assemblies with cyclic symmetry part I:
627 free vibrations[J]. Journal of Vibration, Acoustics, Stress, and Reliability in Design, 1988, 110(4): 429-
628 438.

629 17. Fang, X., et al., Crack induced vibration localization in simplified bladed-disk structures. Journal
630 of Sound and Vibration, 2006. 291(1-2): p. 395-418.

631 18. Castanier, M.P. and C. Pierre, Modeling and Analysis of Mistuned Bladed Disk Vibration:
632 Current Status and Emerging Directions. Journal of Propulsion and Power, 2006. 22(2): p. 384-396.

633 19. Valentín, D., et al., Experimental Study of a Vibrating Disk Submerged in a Fluid-Filled Tank
634 and Confined With a Nonrigid Cover. Journal of Vibration and Acoustics, 2017. 139(2).

635 20. Castanier, M.P. and C. Pierre, Using Intentional Mistuning in the Design of Turbomachinery
636 Rotors. AIAA Journal, 2002. 40(10): p. 2077-2086.

637 21. Wang J J, L.Q.H., Methods and Applications of reduction modeling for mistuned bladed disk
638 vibration in aero-engine. 2009: Nation Defense Industry Press, China.

639 22. Saeed, R.A., A.N. Galybin, and V. Popov, 3D fluid-structure modelling and vibration analysis
640 for fault diagnosis of Francis turbine using multiple ANN and multiple ANFIS. Mechanical Systems
641 and Signal Processing, 2013. 34(1-2): p. 259-276.

642 23. Liu, R., et al., Artificial intelligence for fault diagnosis of rotating machinery: A review.
643 Mechanical Systems and Signal Processing, 2018. 108: p. 33-47.